Journal Pre-proof

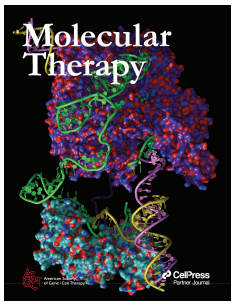

Lipid Nanoparticle Delivery of TALEN mRNA Targeting *LPA* Causes Gene Disruption and Plasma Lipoprotein(a) Reduction in Transgenic Mice.

Daniel A. Garcia, Abigail F. Pierre, Linda Quirino, Grishma Acharya, Aishwarya Vasudevan, Yihua Pei, Emily Chung, Jason Y.H. Chang, Samuel Lee, Michael Endow, Kristen Kuakini, Michael Bresnahan, Maria Chumpitaz, Kumar Rajappan, Suezanne Parker, Padmanabh Chivukula, Stefen A. Boehme, Ramon Diaz-Trelles

PII: S1525-0016(24)00747-0

DOI: https://doi.org/10.1016/j.ymthe.2024.11.020

Reference: YMTHE 6641

To appear in: *Molecular Therapy*

Received Date: 26 February 2024

Accepted Date: 15 November 2024

Please cite this article as: Garcia DA, Pierre AF, Quirino L, Acharya G, Vasudevan A, Pei Y, Chung E, Chang JYH, Lee S, Endow M, Kuakini K, Bresnahan M, Chumpitaz M, Rajappan K, Parker S, Chivukula P, Boehme SA, Diaz-Trelles R, Lipid Nanoparticle Delivery of TALEN mRNA Targeting *LPA* Causes Gene Disruption and Plasma Lipoprotein(a) Reduction in Transgenic Mice., *Molecular Therapy* (2024), doi: https://doi.org/10.1016/j.ymthe.2024.11.020.

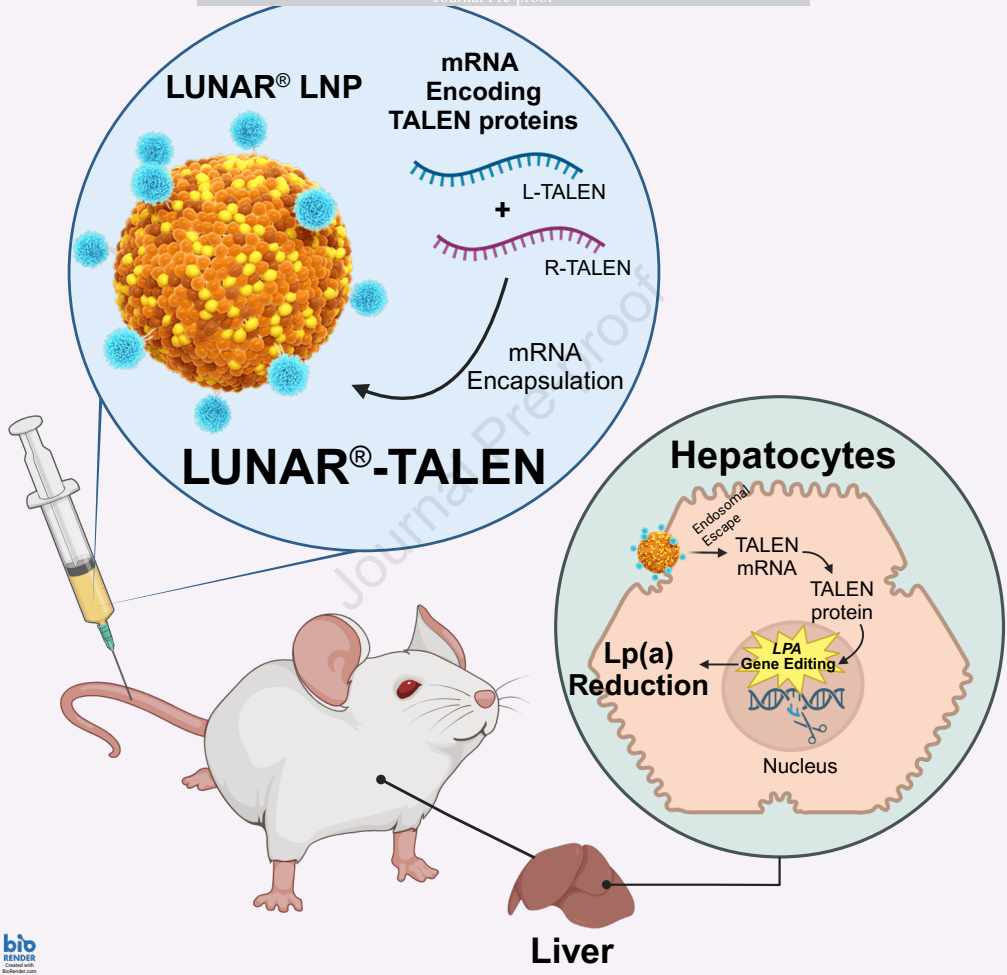

Lipid Nanoparticle Delivery of TALEN mRNA Targeting *LPA* Causes Gene Disruption and Plasma Lipoprotein(a) Reduction in Transgenic Mice.

Daniel A. Garcia*, Abigail F. Pierre, Linda Quirino, Grishma Acharya, Aishwarya Vasudevan, Yihua Pei, Emily Chung, Jason Y. H. Chang, Samuel Lee, Michael Endow, Kristen Kuakini, Michael Bresnahan, Maria Chumpitaz, Kumar Rajappan, Suezanne Parker, Padmanabh Chivukula, Stefen A. Boehme*, Ramon Diaz-Trelles

Arcturus Therapeutics, Inc., 10628 Science Center Drive, Suite 250, San Diego, CA 92121, USA

* To whom correspondence should be addressed. Email: danielg@arcturusrx.com, stefen@arcturusrx.com

SHORT TITLE (50 chars or less, including spaces)

TALEN-mediated gene editing for Lp(a) reduction

ABSTRACT

Lipoprotein(a), or Lp(a), is encoded by the *LPA* gene and is a causal genetic risk factor for cardiovascular disease. Individuals with high Lp(a) are at risk for cardiovascular morbidity and are refractory to standard lipid-lowering agents. Lp(a)-lowering therapies currently in clinical development require repetitive dosing, while a gene editing approach presents an opportunity for a single-dose treatment. In this study, mRNAs encoding Transcription Activator-Like Effector Nucleases (TALENs) were designed to target human *LPA* for gene disruption and permanent Lp(a) reduction. TALEN mRNAs were screened *in vitro* and found to cause on-target gene editing and target protein reduction with minimal off-target editing. TALEN mRNAs were then encapsulated with LUNAR®, a proprietary lipid nanoparticle (LNP), and administered to transgenic mice that expressed a human *LPA* transgene. A single dose of TALEN mRNA-LNPs reduced plasma Lp(a) levels in mice by over 80%, which was sustained for at least 5 weeks. Moreover, both standard and long-read next generation sequencing confirmed the presence of gene-inactivating deletions at *LPA* transgene loci. Overall, this study serves as a proof-of-concept for using TALEN-mediated gene editing to disrupt *LPA in vivo*, paving the way for the development of a feasible gene editing therapy for patients with high Lp(a).

INTRODUCTION

Lipoprotein(a), or Lp(a), is a low-density lipoprotein (LDL)-like lipoprotein with the addition of apolipoprotein(a) (apo(a)) protein covalently bound to apolipoprotein B-100 (apoB-100).[1] While LDL levels can be controlled with various pharmaceutical interventions, Lp(a) levels are refractory to statins and other lipid-lowering therapies.[2–4] It is well-established that individuals with high levels of Lp(a) in their blood are at higher risk for major cardiovascular events and mortality.[5–7] Considering that an estimated 1.4 billion individuals worldwide with high Lp(a) (≥50 mg/dL) are at higher risk for atherosclerotic cardiovascular disease and calcific aortic valve disease, this presents a critical population health burden and an unmet medical need.[8]

Apo(a) is encoded by the *LPA* gene in humans and its expression is restricted to the liver where it is assembled into Lp(a) and secreted into the circulation.[9] Lp(a) levels are inversely related to the number of Kringle IV type 2 (KIV-2) domain repeats present in apo(a), with smaller isoforms more efficiently exported by hepatocytes resulting in higher circulating Lp(a) levels.[10,11] RNA-targeting therapies aimed at lowering Lp(a) are currently in development and show great potential for clinical success.[12] For instance, ongoing clinical trials for siRNA- and ASO-based therapeutics can lower Lp(a) in patients by up to 97% after a single dose.[13–15] However, siRNA and ASO therapeutics are limited by the need for long-term repeat administration to maintain low Lp(a) levels, raising potential tolerability and safety concerns. This presents an opportunity for a gene editing therapeutic approach that can permanently lower Lp(a) after a single administration. Indeed, this approach is being pursued by multiple pharmaceutical companies using various Clustered Regularly Interspaced Short Palindromic Repeats (CRISPR)-Cas9-based platform technologies. Importantly, a CRISPR-Cas9 approach for

LPA gene editing has recently been validated in proof-of-concept studies in transgenic mice using AAV-based delivery.[16] While a CRISPR-Cas9 gene editing approach is feasible for *LPA*, AAV-based delivery presents various risks that prevent it from being developed further clinically, such as immunogenicity that can preclude repeat dosing if necessary, chromosomal integration of the vector, and increased off-target risk due to continuous expression of Cas9.

mRNA encoded Transcription Activator Like Effector Nucleases (TALENs) represent an alternative therapeutic genome editing tool. TALENs are derived from Transcription Activator-like Effectors (TALEs) which are naturally occurring proteins found in *Xanthomonas*, a common plant bacterial pathogen.[17,18] TALENs contain a DNA-binding domain – customized to target any DNA sequence in the genome – linked to an effector domain consisting of the obligate dimer FokI nuclease.[19] Specific DNA sequence targeting by TALENs is designated by the modular assembly of repeat variable di-residue (RVD) domains, each of which recognizes a single specific DNA base (Fig. 1A). TALENs perform gene editing at specific sites in a pairwise fashion, since the FokI nuclease is an obligate dimer. Therefore, two different TALEN monomers (left and right) are designed for a given target site, each binding a separate sequence on opposite DNA strands of the target cut site (Fig. 1A). Gene editing occurs when the FokI nuclease dimer cleaves target DNA leading to the efficient induction of insertions and deletions (indels) by non-homologous end joining (NHEJ) repair of double-strand DNA breaks. Indels introduced by NHEJ result in frameshift mutations, premature stop codons and gene disruption.

While CRISPR-Cas9 and its various nuclease derivatives demonstrate robust DNA cleavage efficiency and design simplicity, TALENs offer distinct advantages as a therapeutic gene editing platform. TALENs can target virtually any DNA sequence since its design is not restricted by protospacer adjacent motif (PAM) sequence requirements, allowing more target

flexibility.[18] TALENs are thought to be inherently more specific, since their targeting sites are larger (30-40 bases) which would be expected to lead to fewer off-target effects.[20] The chromatin environment has also been shown to be an important factor for gene editing activity, where TALENs exhibited greater editing efficiency compared to CRISPR-Cas9 in regions of heterochromatin.[21] Interestingly, *LPA* contains various regions of heterochromatin, suggesting TALENs are more suited for this target than CRISPR-based strategies.

Although *in vivo* delivery of genome editing therapies has been a challenge, the recent proven success of mRNA vaccines has encouraged the development of other *in vivo* mRNA therapies utilizing lipid nanoparticle (LNP)-based delivery.[22–25] For example, the first LNP-based CRISPR-Cas9 *in vivo* gene editing therapy was recently tested in humans for the rare disease hereditary transthyretin amyloidosis, or hATTR.[26] We propose the use of TALEN mRNAs to target the *LPA* gene *in vivo* using LUNAR®, a proprietary LNP-based mRNA delivery platform. LUNAR® LNPs are comprised of a proprietary ionizable lipid, a phospholipid, cholesterol, and polyethylene glycol (PEG), and are designed to be biodegradable, well-tolerated, and optimized for liver delivery due to their LDL receptor-mediated cellular uptake in hepatocytes.[27–31]

In this study, therapeutic mRNAs encoding TALEN gene editing proteins were designed and tested *in vitro* for *LPA* gene editing and off-target activity. The *in vivo* delivery and subsequent plasma Lp(a) reduction of a pair of TALEN mRNAs encapsulated by LUNAR® LNPs (LUNAR®-TAL$_1$) was tested in Lp(a) transgenic mice, and the gene-disrupting deletions were characterized. Overall, we demonstrate for the first time the delivery of TALEN mRNAs *in vivo* using LUNAR® LNP technology providing a proof-of-concept for *LPA* gene editing *in vivo* and efficacious Lp(a)-lowering with a single dose.

RESULTS

TALENs targeting *LPA* reduce apo(a) protein and result in *LPA* gene editing *in vitro*.

Two TALENs (TAL_1 and TAL_2) were designed to target separate loci in the *LPA* gene (Fig. 1B). TAL_1, which binds in the KIV-2 domain of *LPA*, was designed with the Paired TALEN Targeter bioinformatic webtool.[32,33] Two separate expression plasmids were created for the TALEN pair, referred to as L-TAL_1 and R-TAL_1. TAL_2, which binds in the KIV-4 domain of *LPA*, is an off-the-shelf pre-designed TALEN, consisting of a pair of plasmid clones referred to as L-TAL_2 and R-TAL_2 (GeneCopoeia, Inc., Rockville, MD). The pre-designed TAL_2 ORFs were subcloned into expression plasmids. All TALEN mRNAs were approximately 4 kb in length, contained a nuclear localization sequence (NLS), 5'- and 3'-untranslated region (UTR) sequences, and a 3xFLAG tag for protein detection (Fig. 1C). mRNAs were produced by IVT and purified with silica columns (see Materials and Methods for details).

We first sought to determine the efficacy of gene editing and target protein reduction of the designed TAL_1 and TAL_2 *in vitro*. L- and R-TAL mRNA pairs were transfected simultaneously into human RT4 cells, an immortalized human bladder carcinoma cell line that expresses *LPA* and produces apo(a) protein.[34] TAL_1 and TAL_2 protein expression and nuclear localization were observed by immunofluorescence 16 hours post-transfection, suggesting the exogenous mRNAs are internalized and lead to protein production in cells (Fig. 2A). TAL_1 and TAL_2 protein expression was further verified by either in-cell western assay or western analysis of whole cell lysates (Fig. S1A-B). At 5 days post-transfection, both TAL_1 and TAL_2 significantly reduced *LPA* transcript expression compared to mock transfected negative control cells in a dose-dependent manner, suggesting TALEN proteins caused *LPA* gene disruption (Fig.

2B). *LPA* transcript reduction translated to a similar level of apo(a) protein reduction observed in western analysis of whole cell lysates (Fig. 2C-D). Dose-dependent gene editing was also observed at each TALEN's respective target loci, demonstrating that *LPA* transcript and apo(a) protein reduction are indeed TALEN-mediated (Fig. 2E). Further, the locations of TALEN-mediated indels confirmed that the majority of gene-disrupting indels are found between the binding sites of the L- and R-TALEN pairs (Fig. S1C-D). Interestingly, TAL_1 exhibited approximately 2.5-fold higher gene editing efficacy than TAL_2 (Fig. 2E). This could be explained, in part, by the multiple TAL_1 target sites present in *LPA* (Fig. 1B). Since TAL_1 performed better than TAL_2, perhaps in part due to more potential target sites, we selected TAL_1 as the lead candidate to move forward in subsequent studies.

Optimized TAL_1 exhibits enhanced efficacy *in vitro*.

We next sought to improve the efficacy of TAL_1 by optimizing the sequence design of the mRNA for maximal protein expression (Fig. 2F). To enhance ribosome recruitment, the 5' UTR was optimized for liver expression. To increase the efficiency of protein translation, we used a proprietary algorithm to optimize codon usage within the ORF sequence for human cells. To augment TALEN FokI nuclease activity, the C-terminal domain was shortened from 63 to 40 amino acids.[35] These changes were incorporated into L-TAL_1 and R-TAL_1 expression plasmids, and are together referred to as TAL_1-opt.

Optimized TAL_1-opt mRNAs transfected in RT4 cells led to a 4-fold increase in TAL_1 protein expression compared to un-optimized TAL_1 mRNA, suggesting that the UTR and codon optimization improved mRNA translation (Fig. 2G). Importantly, this correlated with an

approximately 50% increase in gene editing compared to un-optimized TAL_1 and corresponding apo(a) protein reduction in whole cell lysates (Fig. 2H-I). To determine the potential for *in vivo* translation of TALEN-mediated gene editing, optimized TAL_1-opt mRNAs were transfected in primary human hepatocytes, which are typically used as *in vitro* surrogates for *in vivo* therapeutic activity. Dose-dependent TAL_1-opt protein expression was observed with in-cell western assay 16 hours post-transfection, showing that primary human hepatocytes can effectively translate TAL_1-opt mRNAs into TALEN proteins (Fig. 2J). Five days after transfection in primary human hepatocytes, we found that TAL_1-opt mRNAs caused significant apo(a) protein reduction in whole cell lysates and up to 60% gene editing in a dose-dependent manner (Fig. 2K-L). Together, these data suggest that TAL_1-opt mRNAs can be efficiently translated into TALEN proteins and mediate gene editing at specific human genomic loci. Furthermore, these data support the importance of mRNA sequence design optimization to improve protein translation and enzymatic activity for efficacy enhancements.

TAL_1 causes minimal off-target editing at sites predicted *in silico*.

Since editing outside of the designed target site is a significant safety concern for gene editing therapeutics, we next sought to determine the specificity of TAL_1. To evaluate potential off-target editing, we identified the top off-target genomic loci using the target prediction webtool TAL Effector Nucleotide Targeter (TALE-NT).[32,33] TALE-NT-predicted targets for TAL_1 consisted of the originally designed canonical on-target site in the KIV-2 domain of *LPA* (LPA-KIV2), two off-target sites within the KIV-3 and KIV-4 domains of *LPA* (LPA-KIV3 and LPA-KIV4), and various other candidate off-target genomic loci (Table S1). Off-target sites are

characterized by a TAL probability binding score of <18.69, a spacer length of 10-30 nt between TALEN monomers, and various mismatches ranging from 3 to 8 nucleotides at either the left or right binding site (Table S1).

We then determined if TAL_1-opt mRNA delivered to cells resulted in gene editing at *in silico* predicted off-target sites. RT4 cells were transfected with a range of TAL_1-opt mRNA doses and gDNA was isolated 5 days later. Interestingly, we found dose-responsive gene editing of up to 30% at alternative target sites within *LPA* (LPA-KIV3, LPA-KIV4), likely due to the sequence homology of those loci with the on-target site, LPA-KIV2 (Fig. S2). This is evident in the TAL scores of each individual TAL_1 monomer at those sites (Table S1). Off-target analysis of 18 total candidate sites (OT1-OT18) revealed no evidence of editing at most sites. Minimal editing was observed (<1.7%) at OT8 and OT16 in the highest TAL_1-opt mRNA dose level (312 pM) (Fig. S2, Table S1). These data suggest that the high efficacy seen for TAL_1-opt may be due to gene editing occurring at three unique sites within the *LPA* gene increasing the probability of gene disruption, and that off-target editing outside of *LPA* is minimal in human cells.

TALEN mRNA-LNPs durably reduce Lp(a) in transgenic mice and are well-tolerated.

To deliver TALEN mRNAs *in vivo*, we developed an LNP delivery system, LUNAR®, that efficiently encapsulates mRNA cargo for protection from nuclease-mediated degradation in the circulation and mediates delivery to the liver.[27–31] TALEN mRNAs (L-TAL_1-opt and R-TAL_1-opt) were encapsulated in LUNAR® LNPs to produce LUNAR®-TAL_1 for *in vivo* intravenous delivery of *LPA*-targeted gene editing therapy (Fig. 3A).

To evaluate LUNAR®-TAL$_1$ gene editing efficacy *in vivo*, we used an Lp(a) double transgenic mouse model that contains a human *LPA* transgene driven by the *APOE* promoter and a human *APOB-100* transgene driven by its endogenous promoter (Fig. 3B). Since mice naturally lack *LPA*, the presence of both human transgenes allows mouse hepatocytes to produce human Lp(a) in the circulation replicating human Lp(a) physiology in a tractable animal model.[36,37] Upon validating the *LPA* transgene sequence by Sanger sequencing primer walk (data not shown), we confirmed the presence of two TAL$_1$ target sites (Fig. 3B). The most upstream site corresponds to the originally designed "canonical" target in the KIV-2 domain (Fig. 3B, purple marker). The downstream site corresponds to the KIV-4 domain in *LPA* (Fig. 3B, red marker), a secondary region where TAL$_1$ was also found to cause editing in human cells (Fig. S2, Table S1). While TAL$_1$ was also found to cause editing in the KIV-3 domain in human cells, that site is not present in the *LPA* transgene sequence. Therefore, TAL$_1$-mediated gene editing could occur at two sites in this mouse model, the KIV-2 domain and the KIV-4 domain (Fig. 3B; TAL$_1$ Target Site 1 and TAL$_1$ Target Site 2, respectively).

Transgenic mice were dosed with 0.5 or 2 mg/kg of LUNAR®-TAL$_1$ either once (1X) or twice (2X, 3 weeks apart), and plasma samples were examined weekly for Lp(a) levels (Fig. 3C). After a single 2 mg/kg dose, Lp(a) levels in plasma were reduced by 80-90% within 7 days (Fig. 3D and Fig. S3A). This significant reduction of Lp(a) was sustained throughout the course of the study, up to 35 days after dosing. Mean Lp(a) levels were also further reduced after a second dose of LUNAR®-TAL$_1$, although the effect was not statistically significant as compared to a single dose (Fig. 3D). However, upon examining the Lp(a) levels of individual mice, we found that mice with a smaller reduction of Lp(a) after the first dose did experience a further reduction in plasma Lp(a) after a second dose of LUNAR®-TAL$_1$ (Fig. S3A). After study termination at 49

days post-dosing, target reduction was also observed in the liver at the transcript level with RT-qPCR (Fig. 3E). Neither plasma Lp(a) nor *LPA* transgene expression in the liver was significantly reduced in mice that were treated with 0.5 mg/kg LUNAR®-TAL1 (Figs. 3D-E and S3A). Overall, these data demonstrated the highly durable efficacy of LUNAR®-TAL1 in reducing Lp(a) levels in the circulation of transgenic mice.

To determine the safety and tolerability of LUNAR®-TAL1, we examined animal body, liver, kidney, and spleen weights, and plasma alanine transaminase (ALT) levels at study termination 49 days after the initial dose. Since minimal Lp(a) reduction was observed for the 0.5 mg/kg group, we focused our safety and tolerability assessment on the 2 mg/kg dose groups only. No significant changes in plasma ALT or organ weights were found, and body weights remained unchanged throughout the course of the study (Figs. 3F and S3B-E). In addition, no significant histopathological findings in H&E-stained liver, kidney, and spleen sections were observed (Fig. S3F), together suggesting that LUNAR®-TAL1 formulations were safe and well-tolerated. Furthermore, no significant reductions were detected in either plasma ApoB-100 or plasminogen – a highly homologous gene to apo(a) – further supporting the target specificity of LUNAR®-TAL1 (Fig. 3G-H). Together, these data demonstrate that LUNAR®-TAL1 displays a favorable safety profile *in vivo* while efficiently reducing Lp(a) in the circulation.

TALEN mRNA-LNPs cause *LPA* transgene disruption in transgenic mice.

To evaluate the extent of liver gene editing in transgenic mice that received LUNAR®-TAL1 formulations, we first used standard next generation sequencing (NGS) of short amplicons generated from TAL1 target regions in gDNA isolated from mouse liver tissue 49 days post-

dosing. Surprisingly, we found a gene editing level of only 10-15% at Target Site 1 and 5-10% at Target Site 2 (Fig. 4A; purple marker and red marker, respectively). The lower editing level at Target Site 2 is likely due to the decreased TALEN efficacy caused by the 3 sequence mismatches in the L-TAL$_1$ binding region at that site (Fig. 4B-C, Table S1). Further, we found the amount of editing between the single and double dose groups was comparable, in alignment with the similar levels of plasma Lp(a) at 35 days post-dosing. We hypothesized that the amount of editing we observed was likely an underestimation, considering that >80% reduction of Lp(a) was observed in the circulation of mice that received LUNAR®-TAL$_1$. To determine if additional unanticipated edits along the *LPA* transgene were not detected by amplicon NGS analysis, we employed long-read NGS to capture sequence information along the entire length of the *LPA* transgene. Transgene amplicons ~3.5 kb in length were sequenced with HiFi long-read sequencing technology (PacBio) and upon read alignment we observed that LUNAR®-TAL$_1$ administration also caused ~340 bp deletions between the Target Sites 1 and 2 (Fig. 4D). Thus, in addition to causing small indel gene edits at the two target sites individually, TALENs cleaving DNA simultaneously at both target sites caused a ~340 bp segment of the transgene to be removed and the resulting ends spliced together by non-homologous end joining (NHEJ) DNA repair. LUNAR®-TAL$_1$-mediated editing of the *LPA* transgene can therefore be classified into three types: A) small indels at Target Site 1; B) small indels at Target Site 2; and C) ~340 bp deletion across Target Sites 1 and 2. These three edit types were quantified using bioinformatic analysis of long-read sequencing data, and we found that edit type C was more frequent than edit types A or B (Fig. 4E). Taking all three edit types into account, we found the total amount of gene editing to be ~25-30% (Fig. 4E). These data suggest that the apparent efficacy of

LUNAR®-TAL1-mediated Lp(a) reduction *in vivo* is due to the cumulative nature of the three types of edits observed in the *LPA* transgene.

To evaluate LUNAR® LNP biodistribution, we assessed extrahepatic gene editing of *LPA* in transgenic mice as an indirect readout. Kidney, spleen, lungs, and gonads were harvested from transgenic mice treated with two administration of 2 mg/kg LUNAR®-TAL1 (2X) and standard amplicon NGS was performed on gDNA isolated from tissues. Gene editing was not detected in the *LPA* transgene at either TAL1 Target Site 1 or 2 in non-hepatic tissues, suggesting that LUNAR®-TAL1 distributes primarily to the liver after intravenous administration (Fig. 4F). We next sought to determine which cell types in the liver uptake LUNAR® LNPs. To evaluate cellular distribution of LUNAR® LNPs in the liver, WT mice were treated with mRNA encoding GFP encapsulated in LUNAR® LNPs (LUNAR®-GFP). Liver tissue IHC revealed widespread GFP expression in whole liver sections 24 hours after a single 2 mg/kg intravenous dose (Fig. S4). Upon closer inspection, we found that hepatocytes were the primary cellular targets for LUNAR®-GFP, while endothelial, bile duct, hepatic artery, and various leukocytes remained largely GFP-negative (Fig. S4). Together, these data suggest LUNAR® LNP delivery *in vivo* was liver-specific and hepatic uptake was primarily by hepatocytes.

DISCUSSION

We have developed a novel TALEN-based *in vivo* gene editing therapy, LUNAR®-TAL$_1$, that was designed to edit human *LPA* in hepatocytes. LUNAR®-TAL$_1$ consists of a proprietary liver-tropic lipid nanoparticle delivery system (LUNAR®), carrying a pair of 4kb-long sequence-optimized TALEN mRNAs (L-TAL$_1$-opt and R-TAL$_1$-opt) that target the human *LPA* gene for double strand cleavage causing indels and resulting in gene disruption. In this study, we showed that in human RT4 cells and primary human hepatocytes, transfection of TALEN mRNAs resulted in dose-dependent *LPA* gene editing that caused *LPA* transcript reduction and apo(a) protein reduction. In human *LPA* transgenic mice, LUNAR®-TAL$_1$ was well-tolerated and resulted in significant *LPA* gene editing in the liver and durable reductions of circulating Lp(a), up to 35 days post-dosing.

LPA gene editing efficacy is highly dependent on the targeting sequence, due to the presence of the naturally occurring KIV-2 domain repeats and the internal sequence homology of the adjacent domains (KIV-3 to KIV-10). The most effective TALEN we tested (TAL$_1$) was designed to bind with high fidelity in the KIV-2 repeat region explaining in-part its superior gene editing efficacy over TAL$_2$. TAL$_1$ likely caused double stranded DNA breaks at each of the various KIV-2 repeats present in RT4 cells and primary hepatocytes, leading to more cumulative edits and higher frequency of gene disruption. Furthermore, the TAL$_1$ off-target editing sites we identified within the *LPA* gene (KIV-3 and KIV-4) also help explain its superior editing efficacy over TAL$_2$ (Fig. S2)

Notably, the transgenic mouse model used in this study contained an *LPA* transgene with only one KIV-2 repeat, thereby limiting the number of potential *LPA* gene editing sites compared to human cells *in vitro.*[37] Due to the nature of how the human *LPA* cDNA was produced for the

transgenic mouse model, the TAL_1 off-target site in KIV-4 was preserved while the TAL_1 off-target site in KIV-3 was not.[36,37] Therefore, TAL_1 was predicted to edit at two sites in the *LPA* transgene, which we confirmed experimentally with amplicon NGS and long-read HiFi sequencing.

Upon examining the KIV-4 target site in the *LPA* transgene, we elucidated that there was a perfect sequence match for R-TAL_1 while there were 3 sequence mismatches for L-TAL_1 (Fig. 4B-C, Table S1). These mismatches were tolerated by TAL_1 resulting in editing at this site in the KIV-4 domain of the *LPA* transgene (Target Site 2). This produced 3 types of edits within the *LPA* transgene: A) small indels in the KIV-2 domain (Target Site 1); B) small indels in the KIV-4 domain (Target Site 2); and C) a larger ~340 bp deletion from simultaneous cleavage at both sites. These three types of editing were detected by long-read HiFi sequencing analysis and together account for the significant level of editing and Lp(a) reduction observed.

Interestingly, the level of gene editing we observed can be considered lower than expected compared to other gene editing therapeutics delivered as mRNAs encapsulated in LNPs.[22,24,25,38] However, considering that the LUNAR® LNP used in this study preferentially targets hepatocytes[27] (Fig. S4), and that hepatocytes make up ~50% of the liver,[39] the 25-30% editing we observed in whole liver tissue can be extrapolated to ~50-60% of hepatocytes. Together, this data suggests that significant Lp(a) reduction in circulation can be achieved with only ~50% of *LPA* transgenes disrupted by TALEN-mediated gene editing. The discrepancy between the extent of gene editing and Lp(a) reduction could also be due to the number of *LPA* transgenes present in hepatocytes of Lp(a) transgenic mice, and whether they lead to expression of Lp(a) depending on their genomic integration site. Furthermore, while it is difficult to design a highly specific TALEN site in the *LPA* gene due to the nature of repetitive sequences, multiple

target sites within the *LPA* locus can increase the overall amount of gene-specific editing, demonstrating superior efficacy and specificity of TAL_1. This suggests that a general strategy to increase gene editing efficacy is to target repetitive sequence elements in a gene, increasing the likelihood of gene disruption, since no pathological consequences were observed 49 days after treatment (Fig. 3F-H and S3B-F).

Off-target editing is a significant safety concern when considering an *in vivo* gene editing therapeutic. While an unbiased method for detecting off-target edits was not used in this study, an *in silico* approach was used to determine that the off-target activity of TAL_1 was minimal outside of *LPA* (Fig. S2). The minimal off-target activity of TAL_1 is in contrast to a recent study describing CRISPR-Cas9 targeting *LPA* in transgenic mice using AAV delivery.[16] Doerfler *et al.* found substantial editing at off-target sites, likely due to the sustained CRISPR-Cas9 activity imparted by AAV delivery. The LUNAR® mRNA-LNP delivery platform benefits from a more transient pharmacokinetic and pharmacodynamic profile that, when applied to TALEN delivery *in vivo*, results in fewer opportunities for off-target engagement. Importantly, no candidate off-target sites were identified in plasminogen or other LPA pseudogenes using an *in silico* approach, which supports the target specificity of TAL_1. Similarly, we found that circulating mouse plasminogen was not affected by TAL_1 treatments (Fig. 3H).

Clinical applications of TALEN-based therapeutics have focused on *ex vivo* gene editing of patient cells for allogenic transfer in cancer and hematologic indications.[40] However, delivery of TALENs for gene editing *in vivo* has been a challenge due to the difficulty of simultaneously delivering two separate TALEN monomers needed for proper nuclease function and subsequent gene disruption. For instance, one study demonstrated adenoviral delivery of TALENs in mice where each TALEN arm was packaged separately because they were too large to be included

together in a single adenoviral vector.[41] While adenoviruses and adeno-associated viruses (AAVs) have been shown to be effective delivery vehicles for nucleic acids in humans, they still present significant safety risks.[42–44] This is the first study to our knowledge that demonstrates TALEN-mediated *in vivo* gene editing in the liver utilizing mRNA encoding TALENs encapsulated in LNPs.

It has not escaped our notice that various other FokI variants exist which impart increased nuclease activity and specificity to TALENs.[45] In this study, we employed WT FokI in our TALEN design, whose homodimerization requirement allows for the potential of two L-TALEN or two R-TALEN monomers to pair and cause gene editing at off-target sites. While this type of off-target editing was predicted to occur for TAL_1 (see "Monomer Combo" in Table S1), it is plausible that using a FokI heterodimer mutant (e.g. ELD+KKR) would eliminate this off-target risk.[46,47] Other FokI mutants, "Sharkey" variants, are reported to have enhanced activity and are likely to increase *in vivo* efficacy.[48] However, testing these FokI variants is outside the scope of this proof-of-concept study, and it would be strongly recommended to consider these when selecting a clinical candidate.

As a monogenic risk factor for cardiovascular disease, elevated Lp(a) represents an ideal target for the application for TALEN-mediated *in vivo* gene editing. *LPA*'s restricted expression in the liver makes it amenable for delivery of mRNA encoding gene editing proteins, since established liver targeting delivery systems such as LNPs are available. Furthermore, Lp(a)'s hepatocyte-specific biogenesis would be expected to have limited physiological side effects due to restricted off-tissue expression. Supporting this notion, humans with loss of Lp(a) have no negative physiological effects.[49] Altogether, this study shows for the first time that Lp(a) reduction can be achieved through TALEN-mediated gene editing using LUNAR® LNP-

mediated delivery of encapsulated TALEN mRNAs *in vivo*. Considering the various advantages of TALEN over CRISPR-Cas9, this proof-of-concept study paves the way for the clinical application of TALEN-based *in vivo* gene editing medicines for genetic diseases such as elevated Lp(a).

MATERIAL AND METHODS

TALEN design.

The TALEN open reading frame (ORF) sequence for TAL_1 was designed to target the human *LPA* gene (human genome assembly GRCh38/hg38; chr6:160,531,482-160,664,275) using the TAL Effector-Nucleotide Targeter 2.0 web-based tool.[32,33] We defined a preset TALEN architecture that included a spacer of 15-20 base pairs and an array of repeat variable diresidue (RVD) domains between 15 and 20.[35] The resulting TAL_1 RVD arrays for L-TAL_1 and R-TAL_1 were converted to a DNA sequence ORFs and constructed into separate plasmid clones for mRNA production. The pre-designed TALEN ORFs targeting human *LPA* (TAL_2) were obtained from GeneCopoeia, Inc. (Rockville, MD). TAL_2 ORF sequences were cloned into separate plasmid clones for mRNA production. All plasmid constructs were verified by DNA sequencing. The genomic coordinates for the TAL_1 and TAL_2 target sites are chr6:160,640,757-160,640,810 and chr6:160,601,037-160,601,093, respectively (human genome assembly GRCh38/hg38).

mRNA production.

mRNA was produced as previously described.[27–29] Briefly, linearized plasmids were used as templates for *in vitro* transcription (IVT) reactions with T7 RNA polymerase and N1-methyl-pseudouridine (N1MPU). Chemically modified 5' caps were incorporated co-transcriptionally and the resulting mRNAs were purified with silica columns.

Cell culture.

Unless otherwise noted, all cell culture materials were obtained from Thermo Fisher Scientific (Waltham, MA). RT4 cells (Sigma-Aldrich, St. Louis, MO) were cultured in McCoy's media supplemented with 10% FBS and 1x Antibiotic-Antimycotic. Primary Human Hepatocytes (PHH) were cultured in William's E media with PHH Thawing and Plating Supplement Pack. All cells were maintained at 37°C with 5% CO_2. PHH were handled according to the supplier's instructions. TALEN mRNA transfections were performed in collagen-coated 96-well plates using Lipofectamine MessengerMax by following the manufacturer's instructions. Each transfection condition was performed in triplicate. Reverse transfections were performed with RT4 cells, while forward transfections were performed with PHH 16 hours after plating. PHH media was replenished 1 hour prior to transfection.

In-cell Western and Immunofluorescence microscopy.

In-cell western assays were performed for quantification of TALEN protein expression. At the indicated timepoints, cells were fixed in 4% paraformaldehyde then permeabilized with 0.1% Triton-X solution. After blocking for 90 minutes at room temperature with Intercept Blocking Buffer (LI-COR, Lincoln, NE), cells were incubated with anti-FLAG primary antibodies (Sigma-Aldrich) overnight at 4°C in blocking buffer containing 0.2% Tween. Cells were then washed with PBS containing 0.1% Tween-20 and incubated overnight at 4°C with IRDye-conjugated secondary antibodies (LI-COR) and CellTag stain (LI-COR) diluted in blocking buffer containing 0.2% Tween-20. Cells were then washed, and plates were scanned with the Odyessey CLx Imaging System (LI-COR). ImageStudio software (LI-COR) was used to quantify the anti-FLAG and CellTag signals in each well. The anti-FLAG signal intensity was

406 normalized by the CellTag signal (total cells) for each well and data were plotted as expression
407 level relative to the negative control.

408 For immunofluorescence microscopy, cells were cultured in chambered coverslip slides
409 (Ibidi, Fitchburg, WI) and transfected with mRNAs. At 16 hours after transfection, cells were
410 fixed in 4% paraformaldehyde diluted in PBS for 15 min at room temperature, then stained with
411 Hoechst 33342 solution (Thermo Fisher Scientific) diluted 1:1,000 in 1 × PBS to detect nuclei.
412 Cells were then permeabilized with 0.1% Triton-X solution. After blocking for 90 minutes at
413 room temperature with Intercept Blocking Buffer (LI-COR, Lincoln, NE), cells were incubated
414 with anti-FLAG primary antibodies (Sigma-Aldrich) overnight at 4°C in blocking buffer
415 containing 0.2% Tween. Cells were then washed with PBS containing 0.1% Tween-20 and
416 incubated with goat anti-mouse Alexa Fluor™ 488 secondary antibodies (Thermo Fisher
417 Scientific) in blocking buffer containing 0.2% Tween-20. Cells were then washed and imaged
418 using the EVOS M5000 Cell Imaging System (Thermo Fisher Scientific). Primary antibody
419 information can be found in the Supplemental Material (Table S6).
420

421 **RT-qPCR**

422 Total RNA was isolated from cultured human cells grown in 96-well plates or mouse
423 liver tissue using the NucleoSpin RNA kit (Macherey-Nagel, Allentown, PA) according to the
424 manufacturer's instructions. Reverse transcription quantitative real-time PCR (RT-qPCR) was
425 performed in technical duplicates using the TaqMan RNA-to-C_T 1-Step Kit (Thermo Fisher
426 Scientific). Gene expression was determined with the $\Delta\Delta C_t$ method using *PPIB* or *Ppia* as the
427 reference gene for human and mouse, respectively, and then normalized relative to the negative
428 control. Primer and probe information can be found in the Supplementary Material (Table S3).

Western Analysis.

Western analysis was performed on cell lysates using the high-throughput capillary electrophoresis Jess instrument (ProteinSimple, San Jose, CA). Cell lysates were prepared on ice from cultured cells in 96-well plates using 80 µL RIPA buffer (Thermo Fisher Scientific) supplemented with Complete EDTA-Free Protease Inhibitor Cocktail tablets (Roche, Basel, Switzerland). After incubation on ice for 20 minutes, lysates were transferred to microcentrifuge tubes and centrifuged at 16,000 x g for 10 minutes at 4°C. Lysate supernatants were then processed by capillary electrophoresis using the standard or high molecular weight separation modules, then probed with primary and secondary antibodies according to the manufacturer's instructions (ProteinSimple). As a loading control, an equal amount of protein was loaded in each well (0.5 µg, as determined by a BCA protein assay) and the Total Protein Detection Module (ProteinSimple) was used to confirm equivalent loading across samples. Primary antibody information can be found in the Supplemental Material (Table S6).

Preparation of lipid nanoparticle formulations.

The LNPs were prepared by mixing lipids in ethanol with mRNA in an acidic aqueous buffer as previously described.[50,51] Briefly, lipid excipients including Arcturus proprietary ionizable lipid, phospholipid, cholesterol, and PEG-DMG were dissolved in ethanol. The lipids were mixed, at a mRNA/total lipid weight/weight ratio of 0.037, with mRNA solution prepared in pH 4.0 citrate buffer 1:3 flow rate (ethanol: citrate v/v) using a commercially available mixer (MIVM-1L, Holland Applied Technologies, Burr Ridge, IL) to keep the ethanol percentage constant at 25%. The freshly formed LNPs were stabilized by sequential dilution with phosphate

buffer at pH 6.5, followed by HEPES buffer at pH 8.0. To concentrate the formulation, the diluted formulations were processed with tangential flow filtration (TFF) using PES hollow fiber membrane (100 kDa MWCO, Repligen, Waltham, MA), and further diafiltered with 10x volume of HEPES buffer and concentrated by centrifuging at 2000 RPM for 15-30 minutes in an Amicon® Ultra filtration tube with a100 kD NMWL cellulose membrane (Millipore Sigma, USA). After filtering the formulation with 0.2 μm PES filter, an in-process RNA concentration determination was performed using RiboGreen® assay following vendor (Thermofisher Scientific, USA) protocol, and the formulation concentration was adjusted to the desired concentration by cryoprotectant addition. After sterile filtration, bulk formulation is aseptically filled into glass vials and stored frozen at −70°C. The final particle size and polydispersity index (PDI) were characterized using a Zen3600 (Malvern Instruments, with Zetasizer 7.1 software, Malvern, U.K). A volume of 50 μL of formulations were diluted into 950 μL of Tris buffer at pH = 7.4 and equilibrated to 25 °C prior to analysis in a 1 mL cuvette using the following settings for measurement: material refractive index of 1.5, dispersant viscosity of 1.1 cP, and refractive index of 1.3. Each sample was analyzed for up to 30 runs. Encapsulation efficiency was calculated by determining the unencapsulated mRNA content by measuring the fluorescence intensity (Fi) upon the addition of RiboGreen (Molecular Probes, Eugene, OR, USA) to the LNP and comparing this value to the total fluorescence intensity (Ft) of the RNA content that is obtained upon lysis of the LNPs by 1% Triton X-100, where % encapsulation = (Ft − Fi)/Ft × 100). The mRNA purity characterization by capillary electrophoresis using fragment analyzer (Agilent Technologies, Santa Clara, CA). All formulations showed encapsulation efficiencies and mRNA purity greater than 90%, particle sizes in the range of 60 to 70 nm, and polydispersity indices under 0.2 (Table S2). While zeta potential was never measured, it is expected to be

within +5 to -5 mV due to the apparent pKa of 6.25 of the ionizable lipid (as measured by a standard TNS assay) and its storage in a buffer with a pH of 8.0. Under these conditions, the LUNAR® LNPs are charge neutral.

Animals

All procedures for animal experimentation were approved by the Arcturus Institutional Animal Care and Use Committee and conducted in accordance with their guidelines. Lp(a) transgenic mice used in this study are previously described.[37] Briefly, Lp(a) mice were produced by crossing human apo(a)-expressing transgenic mice with human apoB-100 transgenic mice. Human apo(a) mice were generated using a human apo(a) cDNA encoding KIV-1, 1 copy of KIV-2, a fusion of KIV-3 and KIV-5, KIV-6 to KIV-10, KV, and the protease-like domain, as described previously.[36,37] Human apoB-100 mice were generated as described previously.[52] The *LPA* transgene sequence was verified by Sanger sequencing primer walk and confirmed the presence of the TAL_1 target sites. LUNAR®-TAL_1 LNPs were administered to mice via lateral tail vein injection at a dose of either 0.5 mg/kg or 2 mg/kg in a volume of 10 mL/kg. Negative control animals were dosed with PBS. Blood was collected in K-EDTA tubes (Sigma-Aldrich) at the indicated timepoints by retroorbital bleeding, and plasma was separated by centrifugation. At the final timepoint, mice were euthanized, and blood was collected via cardiac puncture for plasma analysis. Liver tissue was weighed and separated for analyses; a 20 mg piece was used for gDNA extraction, and the medial lobe was fixed in formalin for histopathology.

Plasma analysis.

Mouse plasma was separated from whole blood by centrifugation after collection in K-EDTA tubes. Plasma levels of ALT were determined using a Vet Axcel Chemistry Analyzer instrument (Alfa Wasserman Diagnostic Technologies, West Caldwell, NJ). Human Lipoprotein(a) levels in plasma were determined using an isoform-independent custom sandwich ELISA.[53,54] Human apolipoprotein(a) levels in plasma were determined with the Human Lipoprotein A ELISA kit (Abcam, Cambridge, UK) using samples diluted to a final concentration of 1:10,000 in sample diluent. Human apolipoprotein B-100 protein levels in mouse plasma were determined with the Human ApoB-100 ELISA kit (Thermo Fisher Scientific) using samples diluted to a final concentration of 100,000-fold with sample diluent. Plasminogen levels in plasma were determined with the Plasminogen Total Mouse ELISA kit (Abcam) using samples diluted to a final concentration of 10,000-fold with sample diluent. All assays were run in technical duplicates according to the manufacturer's instructions. The technical duplicates were averaged, and the protein concentrations were interpolated using the sigmoidal, 4PL, standard curve method in GraphPad Prism software (Dotmatics, San Diego, CA).

Gene editing quantification using amplicon-based next-generation sequencing (NGS)

Gene editing analysis in cell lines was performed using amplicon-based NGS at Azenta, Inc. (South Plainfield, NJ). Briefly, genomic DNA (gDNA) was isolated from RT4 cells and PHH 5 days post-transfection using the NucleoSpin Tissue kit (Macherey-Nagel) according to the manufacturer's instructions. Target loci were amplified from gDNA templates by PCR using primers containing partial Illumina adapter sequences at the 5' end. Purified PCR products were verified by gel electrophoresis. Library preparation, sequencing, and analysis were performed at

Azenta, Inc. using the Amplicon-EZ next generation sequencing service. Gene editing analysis in mouse liver tissue was performed at GeneGoCell, Inc. (San Diego, CA). Briefly, gDNA was isolated from mouse liver tissue using MagMAX Cell and Tissue DNA Extraction Buffer (Thermo Fisher Scientific) and Proteinase K (GoldBio, St. Louis, MO), followed by the Genomic DNA Clean & Concentrator-25 kit (Zymo Research). Library preparation was conducted following GeneGoCell's proprietary library preparation method. Libraries were sequenced on an NextSeq2000 instrument (Illumina). Analysis was performed using GeneGoCell's G-Amp-MR^{SM} bioinformatics pipeline for NGS. Primer information can be found in the Supplemental Material (Table S4).

Gene editing quantification using amplicon-based long-read NGS

Long-read NGS sequencing was used to identify gene editing along the entire length of *LPA* transgenes in mouse liver tissue. Briefly, genomic DNA from mouse liver tissue was isolated as previously described. Primers were designed to generate 3.6 kb amplicons spanning the *LPA* transgene and PCRs were performed using 100 ng of gDNA template, 10 µM forward and reverse primers (see Table S5 for sequence information), and Platinum SuperFi II PCR Master Mix (Thermo Fisher Scientific) in a total volume of 25 µl. The initial denaturing step occurred at 98 °C for 2 minutes. The samples were then denatured at 98 °C for 15 seconds, annealed at 60 °C for 10 seconds and extended at 72 °C for 2 minutes. This cycle was repeated 35 times. The final elongation step occurred at 72 °C for 5 minutes. Thirty PCR reactions were pooled per animal to meet the starting material requirements for long-read sequencing. Purified amplicons were confirmed by gel electrophoresis and quantified using Qubit dsDNA HS Assay Kit (Thermo Fisher Scientific) used as input for library preparation using SMRTbell Express

Template Prep Kit 2.0 (Pacific Biosciences, Menlo Park, CA). The libraries were then sequenced using the 30-hour movie time on the PacBio Sequel II instrument (Pacific Biosciences) at Molecular Research LP (Shallowater, TX).

Bioinformatic analysis was performed at Monoceros Biosystems, LLC (San Diego, CA). Briefly, long-read sequences from treated and control samples were aligned to the reference sequence (*LPA* transgene sequence) using MiniMap2 v2.23.[55,56] A visual inspection of the aligned reads was done using IGV (2.5.3) to confirm read deletions in treated samples at expected cut point locations. Aligned reads were filtered to remove those reads that didn't span across the expected deletion region using custom code (Python 3.7). The remaining reads after filtering were used to calculate average read coverage across four non-edited positions and the average coverage at two edited positions in order to determine the ratio of read coverage at targeted and non-targeted sites using Samtools Depth (1.15). Reads with deletions spanning the expected cut points (495, 835, or both) were extracted to determine the distribution of deletion lengths in treated and control samples using custom code (Python 3.7).

Histopathology.

Mouse liver medial lobes were excised and fixed in 10% buffered neutral formalin. Tissue processing and microscopy was performed at SDHistoPath (San Diego, CA). Briefly, formalin fixed tissues were paraffin-embedded and cut in 5μm sections that were placed on glass slides for standard H&E staining and immunohistochemistry (IHC). The H&E and IHC images were evaluated for morphological findings by a board-certified pathologist.

Statistical analysis.

All values are presented as mean +/- SEM. GraphPad Prism was used to perform statistical tests. Differences among groups were evaluated using either one-way or two-way ANOVA, where appropriate. Unless otherwise noted, a sample size of n=3 biological replicates was used for all *in vitro* studies and experiments were repeated at least twice. The *in vivo* study was designed to detect a medium effect size (Cohen's d=0.5) with a two-sided confidence interval of 95% (α=0.05) and desired power (1-β) of 80%, requiring a total sample size of three mice per group (n=3). To account for potential animal losses, we therefore determined that n=3 for the negative control group and n=4 for the LUNAR®-TAL$_1$-treated groups were appropriate sample sizes for this study.

DATA AVAILABILITY STATEMENT

All data is available upon request to the corresponding authors.

ACKNOWLEDGEMENTS

We thank Dr. Calvin Yeang (UC San Diego) and his group for their excellent technical services and feedback on *in vivo* study design and operations; the In Vivo Pharmacology, DS Production, DP Formulation, and Translational Biology teams at Arcturus Therapeutics for their technical support; Sourabh Shukla, Claine Snow, and Simone Ward for their critical reading of the manuscript; and our many colleagues at Arcturus Therapeutics for their insightful and helpful discussions.

AUTHOR CONTRIBUTIONS

D.A.G., G.A., S.A.B., K.R., and R.D.T. designed research and wrote manuscript. D.A.G., A.P., L.Q., A.V., Y.P., E.C., J.Y.H.C, S.L., M.E., K.K., M.B., and M.C. performed research. S.P., P.C., K.R., S.A.B., and R.D.T. supervised research.

DECLARATION OF INTERESTS

All authors are paid employees of Arcturus Therapeutics, Inc. All studies were conducted with internal funding from Arcturus Therapeutics, Inc.

KEYWORDS

LUNAR, lipid nanoparticle, LNP, mRNA therapeutics, TALEN, gene editing, Lp(a), Lipoprotein(a), LPA

REFERENCES

1. Schmidt, K., Noureen, A., Kronenberg, F. & Utermann, G. Structure, function, and genetics of lipoprotein (a). *J. Lipid Res.* **57**, 1339–1359 (2016).
2. Reyes-Soffer, G., Ginsberg, H. N., Berglund, L., Duell, P. B., Heffron, S. P., Kamstrup, P. R., Lloyd-Jones, D. M., Marcovina, S. M., Yeang, C., Koschinsky, M. L., *et al.* Lipoprotein(a): A Genetically Determined, Causal, and Prevalent Risk Factor for Atherosclerotic Cardiovascular Disease: A Scientific Statement From the American Heart Association. *Arterioscler. Thromb. Vasc. Biol.* **42**, e48–e60 (2022).
3. Willeit, P., Ridker, P. M., Nestel, P. J., Simes, J., Tonkin, A. M., Pedersen, T. R., Schwartz, G. G., Olsson, A. G., Colhoun, H. M., Kronenberg, F., *et al.* Baseline and on-statin treatment lipoprotein(a) levels for prediction of cardiovascular events: individual patient-data meta-analysis of statin outcome trials. *Lancet Lond. Engl.* **392**, 1311–1320 (2018).
4. Tsimikas, S., Gordts, P. L. S. M., Nora, C., Yeang, C. & Witztum, J. L. Statin therapy increases lipoprotein(a) levels. *Eur. Heart J.* **41**, 2275–2284 (2020).
5. Nordestgaard, B. G. & Langsted, A. Lipoprotein (a) as a cause of cardiovascular disease: insights from epidemiology, genetics, and biology. *J. Lipid Res.* **57**, 1953–1975 (2016).
6. Langsted, A., Kamstrup, P. R. & Nordestgaard, B. G. High lipoprotein(a) and high risk of mortality. *Eur. Heart J.* **40**, 2760–2770 (2019).
7. Patel, A. P., Wang, M., Pirruccello, J. P., Ellinor, P. T., Ng, K., Kathiresan, S. & Khera, A. V. Lp(a) (Lipoprotein[a]) Concentrations and Incident Atherosclerotic Cardiovascular Disease. *Arterioscler. Thromb. Vasc. Biol.* **41**, 465–474 (2021).
8. Kamstrup, P. R. Lipoprotein(a) and Cardiovascular Disease. *Clin. Chem.* **67**, 154–166 (2021).

9. Boffa, M. B. & Koschinsky, M. L. Oxidized phospholipids as a unifying theory for lipoprotein(a) and cardiovascular disease. *Nat. Rev. Cardiol.* **16**, 305–318 (2019).
10. White, A. L., Guerra, B. & Lanford, R. E. Influence of Allelic Variation on Apolipoprotein(a) Folding in the Endoplasmic Reticulum *. *J. Biol. Chem.* **272**, 5048–5055 (1997).
11. Azrolan, N., Gavish, D. & Breslow, J. L. Plasma lipoprotein(a) concentration is controlled by apolipoprotein(a) (apo(a)) protein size and the abundance of hepatic apo(a) mRNA in a cynomolgus monkey model. *J. Biol. Chem.* **266**, 13866–13872 (1991).
12. Dolgin, E. Lp(a)-lowering drugs bolster cardiovascular pipeline. *Nat. Rev. Drug Discov.* **19**, 154–155 (2020).
13. Tsimikas, S., Karwatowska-Prokopczuk, E., Gouni-Berthold, I., Tardif, J.-C., Baum, S. J., Steinhagen-Thiessen, E., Shapiro, M. D., Stroes, E. S., Moriarty, P. M., Nordestgaard, B. G., *et al.* Lipoprotein(a) Reduction in Persons with Cardiovascular Disease. *N. Engl. J. Med.* **382**, 244–255 (2020).
14. O'Donoghue, M. L., G. López, J. A., Knusel, B., Gencer, B., Wang, H., Wu, Y., Kassahun, H. & Sabatine, M. S. Study design and rationale for the Olpasiran trials of Cardiovascular Events And lipoproteiN(a) reduction-DOSE finding study (OCEAN(a)-DOSE). *Am. Heart J.* **251**, 61–69 (2022).
15. Nissen, S. E., Wolski, K., Balog, C., Swerdlow, D. I., Scrimgeour, A. C., Rambaran, C., Wilson, R. J., Boyce, M., Ray, K. K., Cho, L., *et al.* Single Ascending Dose Study of a Short Interfering RNA Targeting Lipoprotein(a) Production in Individuals With Elevated Plasma Lipoprotein(a) Levels. *JAMA* **327**, 1679 (2022).

16. Doerfler, A. M., Park, S. H., Assini, J. M., Youssef, A., Saxena, L., Yaseen, A. B., De Giorgi, M., Chuecos, M., Hurley, A. E., Li, A., *et al.* LPA disruption with AAV-CRISPR potently lowers plasma apo(a) in transgenic mouse model: A proof-of-concept study. *Mol. Ther. Methods Clin. Dev.* **27**, 337–351 (2022).
17. Boch, J. & Bonas, U. Xanthomonas AvrBs3 family-type III effectors: discovery and function. *Annu. Rev. Phytopathol.* **48**, 419–436 (2010).
18. Scott, J. N. F., Kupinski, A. P. & Boyes, J. Targeted genome regulation and modification using transcription activator-like effectors. *FEBS J.* **281**, 4583–4597 (2014).
19. Ousterout, D. G. & Gersbach, C. A. The Development of TALE Nucleases for Biotechnology. *Methods Mol. Biol. Clifton NJ* **1338**, 27–42 (2016).
20. Bhardwaj, A. & Nain, V. TALENs—an indispensable tool in the era of CRISPR: a mini review. *J. Genet. Eng. Biotechnol.* **19**, 125 (2021).
21. Jain, S., Shukla, S., Yang, C., Zhang, M., Fatma, Z., Lingamaneni, M., Abesteh, S., Lane, S. T., Xiong, X., Wang, Y., *et al.* TALEN outperforms Cas9 in editing heterochromatin target sites. *Nat. Commun.* **12**, 606 (2021).
22. Brooks, D. L., Carrasco, M. J., Qu, P., Peranteau, W. H., Ahrens-Nicklas, R. C., Musunuru, K., Alameh, M.-G. & Wang, X. Rapid and definitive treatment of phenylketonuria in variant-humanized mice with corrective editing. *Nat. Commun.* **14**, 3451 (2023).
23. Khera, A., Lee, R., Rohde, E., Jayaram, H., Kathiresan, S. & Bellinger, A. An in vivo CRISPR base editing therapy to inactivate the ANGPTL3 gene: nomination of a development candidate for VERVE-201. *Eur. Heart J.* **43**, ehac544.3087 (2022).

24. Rothgangl, T., Dennis, M. K., Lin, P. J. C., Oka, R., Witzigmann, D., Villiger, L., Qi, W., Hruzova, M., Kissling, L., Lenggenhager, D., *et al.* In vivo adenine base editing of PCSK9 in macaques reduces LDL cholesterol levels. *Nat. Biotechnol.* **39**, 949–957 (2021).
25. Conway, A., Mendel, M., Kim, K., McGovern, K., Boyko, A., Zhang, L., Miller, J. C., DeKelver, R. C., Paschon, D. E., Mui, B. L., *et al.* Non-viral Delivery of Zinc Finger Nuclease mRNA Enables Highly Efficient In Vivo Genome Editing of Multiple Therapeutic Gene Targets. *Mol. Ther.* **27**, 866–877 (2019).
26. Gillmore, J. D., Gane, E., Taubel, J., Kao, J., Fontana, M., Maitland, M. L., Seitzer, J., O'Connell, D., Walsh, K. R., Wood, K., *et al.* CRISPR-Cas9 In Vivo Gene Editing for Transthyretin Amyloidosis. *N. Engl. J. Med.* **385**, 493–502 (2021).
27. Perez-Garcia, C. G., Diaz-Trelles, R., Vega, J. B., Bao, Y., Sablad, M., Limphong, P., Chikamatsu, S., Yu, H., Taylor, W., Karmali, P. P., *et al.* Development of an mRNA replacement therapy for phenylketonuria. *Mol. Ther. Nucleic Acids* **28**, 87–98 (2022).
28. de Alwis, R., Gan, E. S., Chen, S., Leong, Y. S., Tan, H. C., Zhang, S. L., Yau, C., Low, J. G. H., Kalimuddin, S., Matsuda, D., *et al.* A single dose of self-transcribing and replicating RNA-based SARS-CoV-2 vaccine produces protective adaptive immunity in mice. *Mol. Ther. J. Am. Soc. Gene Ther.* **29**, 1970–1983 (2021).
29. Ramaswamy, S., Tonnu, N., Tachikawa, K., Limphong, P., Vega, J. B., Karmali, P. P., Chivukula, P. & Verma, I. M. Systemic delivery of factor IX messenger RNA for protein replacement therapy. *Proc. Natl. Acad. Sci.* **114**, E1941–E1950 (2017).
30. Albers, S., Allen, E. C., Bharti, N., Davyt, M., Joshi, D., Perez-Garcia, C. G., Santos, L., Mukthavaram, R., Delgado-Toscano, M. A., Molina, B., *et al.* Engineered tRNAs suppress nonsense mutations in cells and in vivo. *Nature* **618**, 842–848 (2023).

683 31. Diaz-Trelles, R., Lee, S., Kuakini, K., Park, J., Dukanovic, A., Gonzalez, J. A., Dam, T.,
684 Kim, J. H., Vega, J. B., Sablad, M., *et al.* Lipid nanoparticle delivers phenylalanine ammonia
685 lyase mRNA to the liver leading to catabolism and clearance of phenylalanine in a
686 phenylketonuria mouse model. *Mol. Genet. Metab. Rep.* **32**, 100882 (2022).
687 32. Doyle, E. L., Booher, N. J., Standage, D. S., Voytas, D. F., Brendel, V. P., VanDyk, J. K. &
688 Bogdanove, A. J. TAL Effector-Nucleotide Targeter (TALE-NT) 2.0: tools for TAL effector
689 design and target prediction. *Nucleic Acids Res.* **40**, W117–W122 (2012).
690 33. Cermak, T., Doyle, E. L., Christian, M., Wang, L., Zhang, Y., Schmidt, C., Baller, J. A.,
691 Somia, N. V., Bogdanove, A. J. & Voytas, D. F. Efficient design and assembly of custom
692 TALEN and other TAL effector-based constructs for DNA targeting. *Nucleic Acids Res.* **39**,
693 7879 (2011).
694 34. Karlsson, M., Zhang, C., Méar, L., Zhong, W., Digre, A., Katona, B., Sjöstedt, E., Butler, L.,
695 Odeberg, J., Dusart, P., *et al.* A single–cell type transcriptomics map of human tissues. *Sci.*
696 *Adv.* **7**, eabh2169 (2021).
697 35. Miller, J. C., Zhang, L., Xia, D. F., Campo, J. J., Ankoudinova, I. V., Guschin, D. Y.,
698 Babiarz, J. E., Meng, X., Hinkley, S. J., Lam, S. C., *et al.* Improved specificity of TALE-
699 based genome editing using an expanded RVD repertoire. *Nat. Methods* **12**, 465–471 (2015).
700 36. Koschinsky, M. L., Tomlinson, J. E., Zioncheck, T. F., Schwartz, K., Eaton, D. L. & Lawn,
701 R. M. Apolipoprotein(a): expression and characterization of a recombinant form of the
702 protein in mammalian cells. *Biochemistry* **30**, 5044–5051 (1991).
703 37. Merki, E., Graham, M. J., Mullick, A. E., Miller, E. R., Crooke, R. M., Pitas, R. E., Witztum,
704 J. L. & Tsimikas, S. Antisense Oligonucleotide Directed to Human Apolipoprotein B-100

Reduces Lipoprotein(a) Levels and Oxidized Phospholipids on Human Apolipoprotein B-100 Particles in Lipoprotein(a) Transgenic Mice. *Circulation* **118**, 743–753 (2008).

38. Finn, J. D., Smith, A. R., Patel, M. C., Shaw, L., Youniss, M. R., van Heteren, J., Dirstine, T., Ciullo, C., Lescarbeau, R., Seitzer, J., *et al.* A Single Administration of CRISPR/Cas9 Lipid Nanoparticles Achieves Robust and Persistent In Vivo Genome Editing. *Cell Rep.* **22**, 2227–2235 (2018).
39. Baratta, J. L., Ngo, A., Lopez, B., Kasabwalla, N., Longmuir, K. J. & Robertson, R. T. Cellular organization of normal mouse liver: a histological, quantitative immunocytochemical, and fine structural analysis. *Histochem. Cell Biol.* **131**, 713–726 (2009).
40. Blattner, G., Cavazza, A., Thrasher, A. J. & Turchiano, G. Gene Editing and Genotoxicity: Targeting the Off-Targets. *Front. Genome Ed.* **2**, 613252 (2020).
41. Zhang, S., Li, L., Kendrick, S. L., Gerard, R. D. & Zhu, H. TALEN mediated somatic mutagenesis in murine models of cancer. *Cancer Res.* **74**, 5311–5321 (2014).
42. Suoranta, T., Laham-Karam, N. & Ylä-Herttuala, S. Strategies to improve safety profile of AAV vectors. *Front. Mol. Med.* **2**, (2022).
43. Ertl, H. C. J. Immunogenicity and toxicity of AAV gene therapy. *Front. Immunol.* **13**, 975803 (2022).
44. Colella, P., Ronzitti, G. & Mingozzi, F. Emerging Issues in AAV-Mediated In Vivo Gene Therapy. *Mol. Ther. Methods Clin. Dev.* **8**, 87–104 (2017).
45. Xiao, A., Wu, Y., Yang, Z., Hu, Y., Wang, W., Zhang, Y., Kong, L., Gao, G., Zhu, Z., Lin, S., *et al.* EENdb: a database and knowledge base of ZFNs and TALENs for endonuclease engineering. *Nucleic Acids Res.* **41**, D415-422 (2013).

46. Nakajima, K. & Yaoita, Y. Comparison of TALEN scaffolds in Xenopus tropicalis. *Biol. Open* **2**, 1364–1370 (2013).

47. Schierling, B., Dannemann, N., Gabsalilow, L., Wende, W., Cathomen, T. & Pingoud, A. A novel zinc-finger nuclease platform with a sequence-specific cleavage module. *Nucleic Acids Res.* **40**, 2623–2638 (2012).

48. Guo, J., Gaj, T. & Barbas, C. F. Directed evolution of an enhanced and highly efficient FokI cleavage domain for Zinc Finger Nucleases. *J. Mol. Biol.* **400**, 96–107 (2010).

49. Emdin, C. A., Khera, A. V., Natarajan, P., Klarin, D., Won, H.-H., Peloso, G. M., Stitziel, N. O., Nomura, A., Zekavat, S. M., Bick, A. G., *et al.* Phenotypic Characterization of Genetically Lowered Human Lipoprotein(a) Levels. *J. Am. Coll. Cardiol.* **68**, 2761–2772 (2016).

50. Rajappan, K., Tanis, S. P., Mukthavaram, R., Roberts, S., Nguyen, M., Tachikawa, K., Sagi, A., Sablad, M., Limphong, P., Leu, A., *et al.* Property-Driven Design and Development of Lipids for Efficient Delivery of siRNA. *J. Med. Chem.* **63**, 12992–13012 (2020).

51. Pei, Y., Bao, Y., Sacchetti, C., Brady, J., Gillard, K., Yu, H., Roberts, S., Rajappan, K., Tanis, S. P., Perez-Garcia, C. G., *et al.* Synthesis and bioactivity of readily hydrolysable novel cationic lipids for potential lung delivery application of mRNAs. *Chem. Phys. Lipids* **243**, 105178 (2022).

52. Linton, M. F., Farese, R. V., Chiesa, G., Grass, D. S., Chin, P., Hammer, R. E., Hobbs, H. H. & Young, S. G. Transgenic mice expressing high plasma concentrations of human apolipoprotein B100 and lipoprotein(a). *J. Clin. Invest.* **92**, 3029–3037 (1993).

53. Gonen, A., Yang, X., Yeang, C., Alekseeva, E., Koschinsky, M., Witztum, J. L., Boffa, M. & Tsimikas, S. Generation and characterization of LPA-KIV9, a murine monoclonal antibody binding a single site on apolipoprotein (a). *J. Lipid Res.* **61**, 1263–1270 (2020).

54. Marcovina, S. M., Navabi, N., Allen, S., Gonen, A., Witztum, J. L. & Tsimikas, S. Development and validation of an isoform-independent monoclonal antibody-based ELISA for measurement of lipoprotein(a). *J. Lipid Res.* **63**, 100239 (2022).

55. Li, H. Minimap2: pairwise alignment for nucleotide sequences. *Bioinforma. Oxf. Engl.* **34**, 3094–3100 (2018).

56. Li, H. New strategies to improve minimap2 alignment accuracy. *Bioinformatics* **37**, 4572–4574 (2021).

LIST OF FIGURE CAPTIONS

Figure 1. TALENs targeting human *LPA* gene. A) TALEN protein domain structure. B) Genomic locus of human *LPA* and the binding locations of the designed TALENs, TAL_1 and TAL_2 (L, Left; R, Right). TAL_1 targeted the KIV-2 domain of *LPA* and was custom designed using the TAL Effector-Nucleotide Targeter 2.0 web-based tool.[32,33] Additional binding sites for TAL_1 are indicated by the orange triangles and are due to the KIV-2 domain repeats present in the human reference genome. This illustration depicts the KIV-2 domain repeated seven times. TAL_2 targeted the KIV-4 domain of *LPA*, and is an off-the-shelf prefabricated design from GeneCopoeia, Inc. C) TALEN mRNA sequence design.

Figure 2: *In vitro* screening of *LPA*-targeting TALEN mRNAs. A) Representative immunofluorescence microscopy images of RT4 cells 16 hours after transfection with 312 pM TALEN mRNAs. Scale bar, 75 µm. B) Dose-dependent reduction of LPA transcripts measured by RT-qPCR 5 days after transfection of TALEN mRNAs in RT4 cells. The dotted line represents the LPA expression level in Negative Control mock transfected cells. C-D) Capillary electrophoresis images of Apo(a) protein level in RT4 whole cell lysates 5 days following TAL_1 (C) or TAL_2 (D) mRNA transfection. E) On-target gene editing analysis of RT4 cells 5 days following TALEN mRNA transfection. The frequency of frameshift-causing insertions and deletions (% Editing) was determined by next-generation sequencing (NGS) of PCR amplicons from genomic DNA (gDNA) templates. For each condition, gDNA from n=3 biological replicates was pooled and together used as the template for amplicon NGS gene editing analysis. F) Schematic of TAL_1 mRNA sequence optimization to generate TAL_1-opt. G-I) In-cell western

quantification of TAL_1 protein level (G), representative capillary electrophoresis images of apo(a) protein level in whole cell lysates (H), and on-target gene editing analysis (I) 16 hours after transfection of the optimized versions of TAL_1 mRNAs (TAL_1-opt) in RT4 cells. J-L) In-cell western quantification of TAL_1 protein level (J), representative capillary electrophoresis images of apo(a) protein level in whole cell lysates (K), and on-target gene editing analysis (L) 16 hours after transfection of TAL_1-opt mRNAs in primary human hepatocytes. For C-D and H-K, an equal amount of total protein was loaded in each well (0.5 µg). aa, amino acids; UTR, untranslated region; NLS, nuclear localization sequence.

Figure 3: LUNAR®-TAL_1 administration reduces Lp(a) and is well-tolerated in a transgenic mouse model. A) TAL_1-opt mRNAs encapsulated in LUNAR® LNPs (LUNAR®-TAL_1) were administered intravenously in mice. B) Schematic representation of the human *LPA* and human *APOB-100* transgenes used to create the double transgenic mouse model expressing human Lp(a). The human *LPA* transgene sequence was verified by Sanger sequencing (data not shown) and TAL_1 target sites were confirmed, indicated with purple and red markers. C) Schematic representation of study design. Mixed groups of male and female transgenic mice were given 0.5 or 2 mg/kg of LUNAR®-TAL_1 intravenously either once (1X) or twice (2X, 3 weeks apart). For all groups, plasma was collected at the indicated timepoints, and liver tissue was harvested at study termination (49 days after the first dose). D) Lp(a) levels in plasma determined by a sandwich ELISA using a capture antibody recognizing apoB-100 and detection antibody recognizing apo(a). E) Relative expression of *LPA* transgene in liver tissue determined by RT-qPCR. F) ALT levels in plasma at study termination determined by a clinical analyzer. G) Human APOB-100 levels in plasma determined by ELISA. H) Plasminogen levels in mouse

plasma at 1 day prior to dosing and 35 days after dosing, determined by ELISA. Filled arrows in (D) and (G) correspond to dosing days indicated in (C).

Figure 4: LUNAR®-TAL$_1$ administration in transgenic mice causes *LPA* gene disruption due to deletions at and between TAL$_1$ Target Sites 1 and 2. A) Schematic representation of human *LPA* transgene depicting editing sites for TAL$_1$. Gene editing analysis (% Editing) at the corresponding target sites was determined by standard amplicon next-generation sequencing (NGS). B-C) Schematic representation of TAL$_1$ Target Site 1 (B) and TAL$_1$ Target Site 2 (C) at the DNA sequence level. Colored triangles indicate approximate locations of double strand breaks caused by the FokI nuclease domain of TAL$_1$. Red-shaded squares indicate bases at which there exists a mismatch between the reference sequence and the DNA-binding RVD in TAL$_1$. D) Representative subset of aligned reads generated from HiFi long-read sequencing of *LPA* transgene amplicons. Gray rectangles represent reads from PBS control mice, and purple rectangles represent reads from mice treated twice (2X) with LUNAR®-TAL$_1$ at 2 mg/kg. Black horizontal lines within reads represent sequence deletions. Reads are aligned to the *LPA* transgene schematic above with TAL$_1$ target sites depicted. E) Gene editing analysis generated from bioinformatic analysis of HiFi sequencing data. "% Editing" indicates indel frequency as a percentage of total read coverage at the indicated target site. "Across Both" indicates deletions that span across both target sites. F) Extrahepatic gene editing determined by standard amplicon NGS of the *LPA* transgene at the indicated target sites. Genomic DNA was isolated from liver, kidney, spleen, lung and gonads of mice treated with two administrations of LUNAR®-TAL$_1$ at 2 mg/kg (2X).

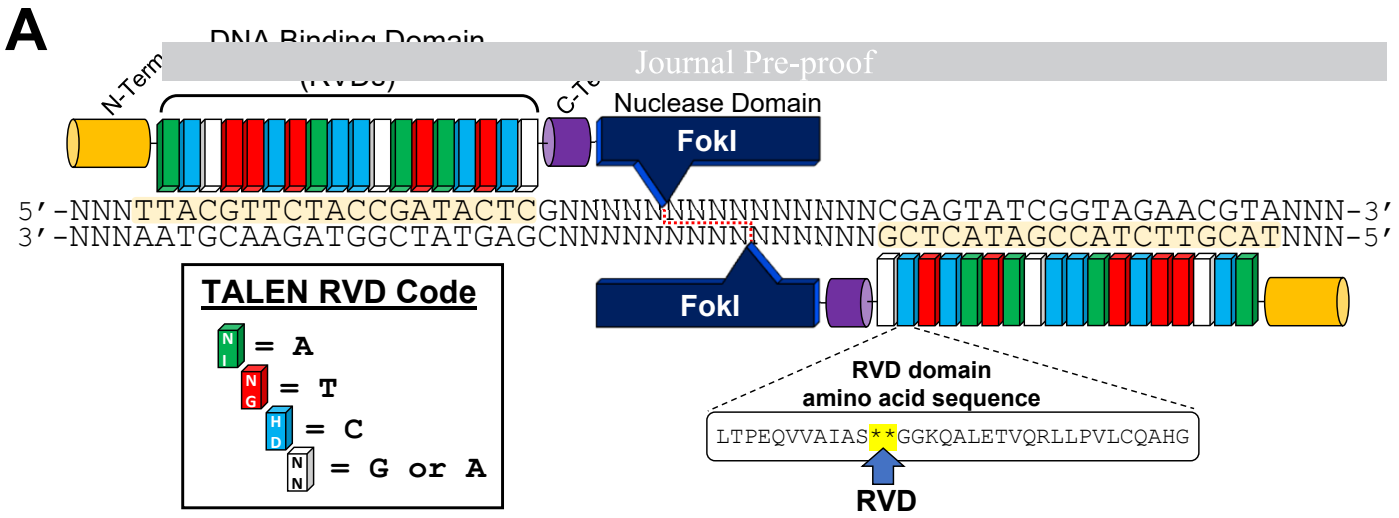

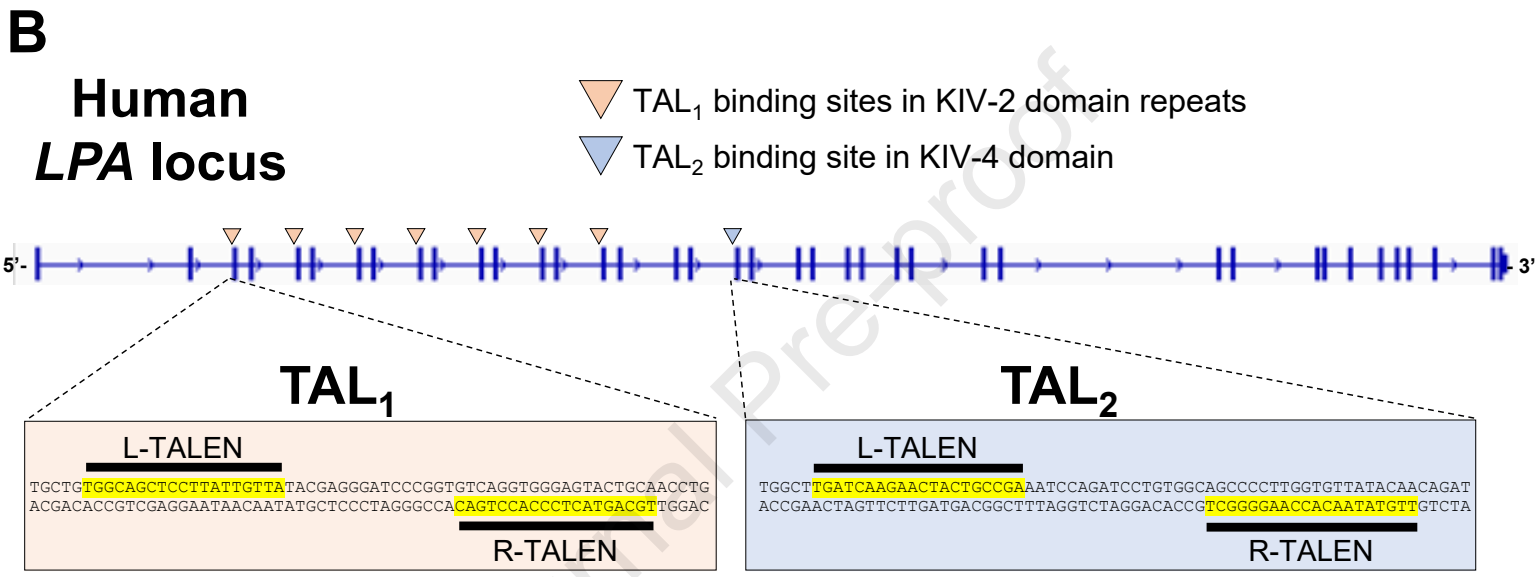

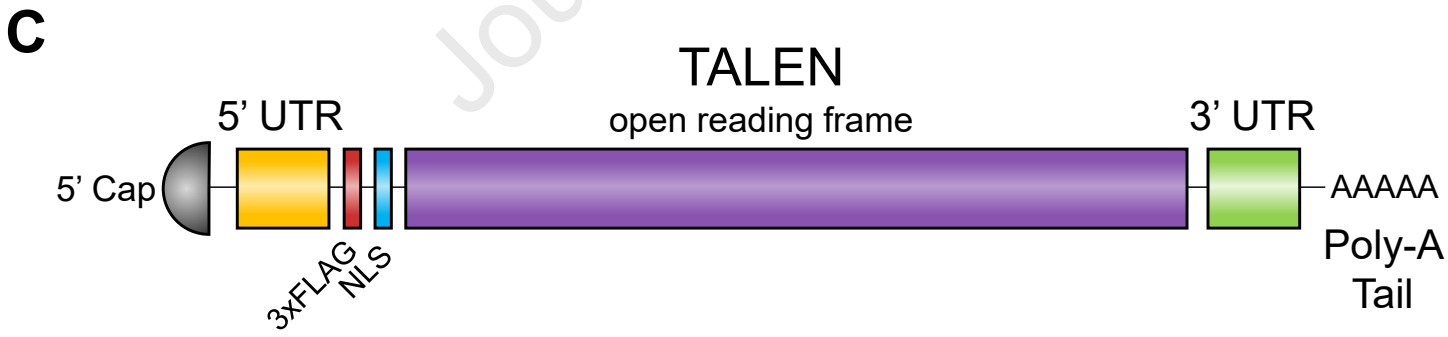

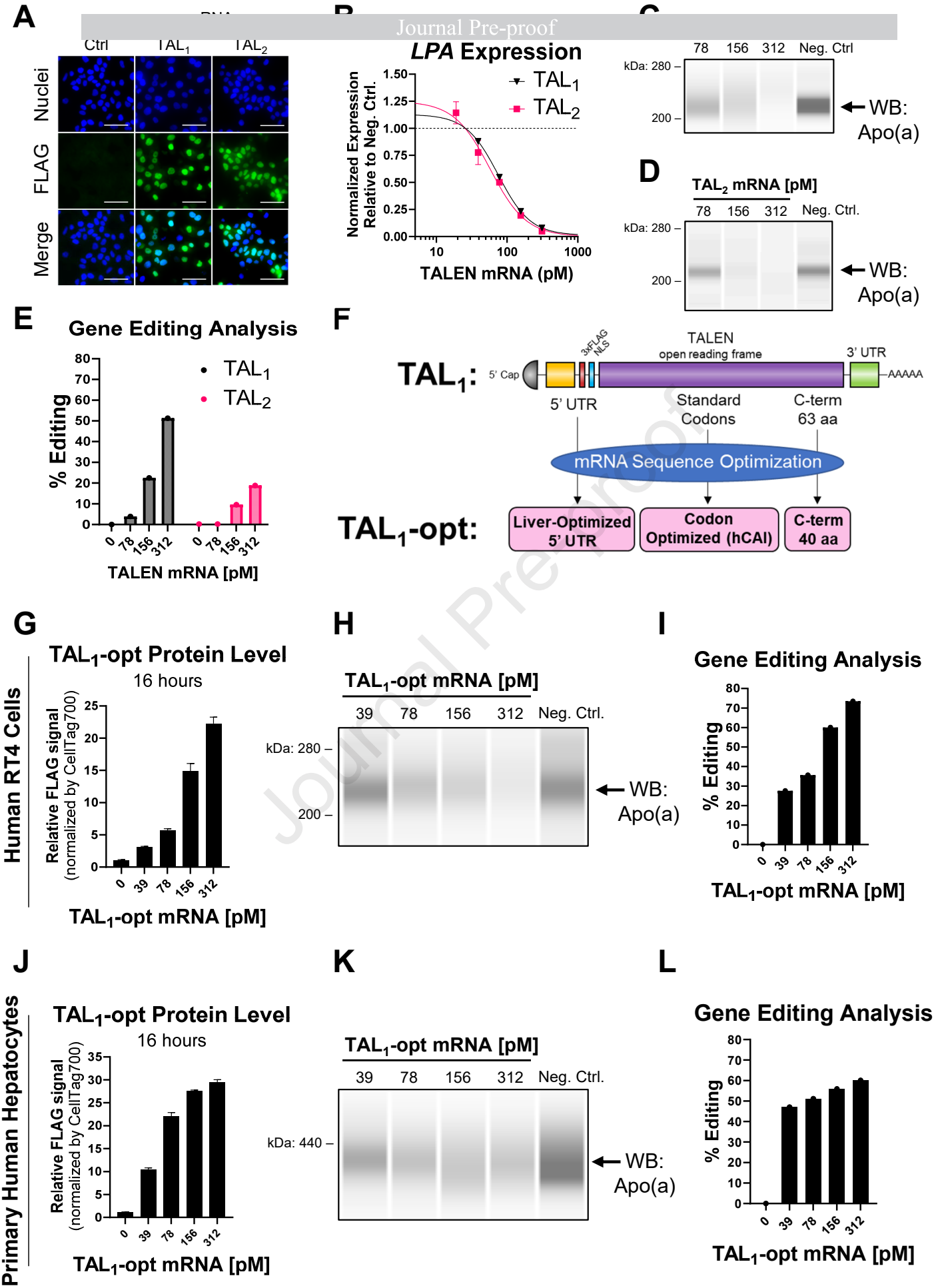

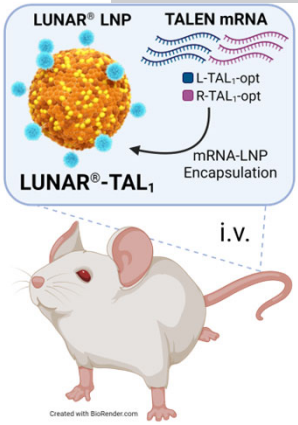

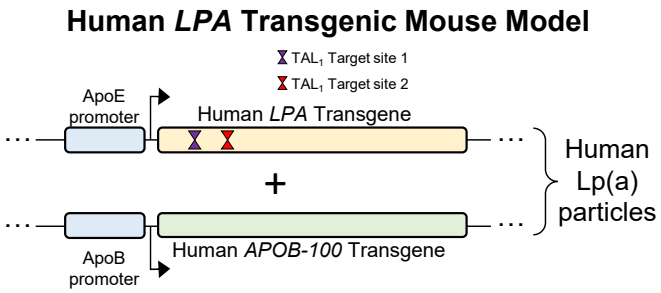

			Freq.	N
1	PBS	-	1X	3
2	LUNAR®-TAL1	0.5 mg/kg	1X	4
3	LUNAR®-TAL1	2 mg/kg	1X	4
4	LUNAR®-TAL1	2 mg/kg	2X	4

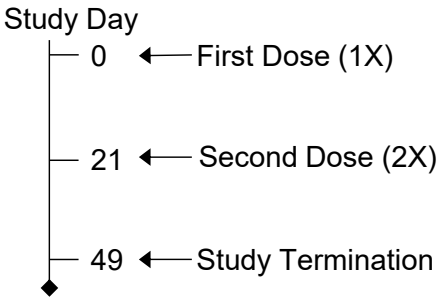

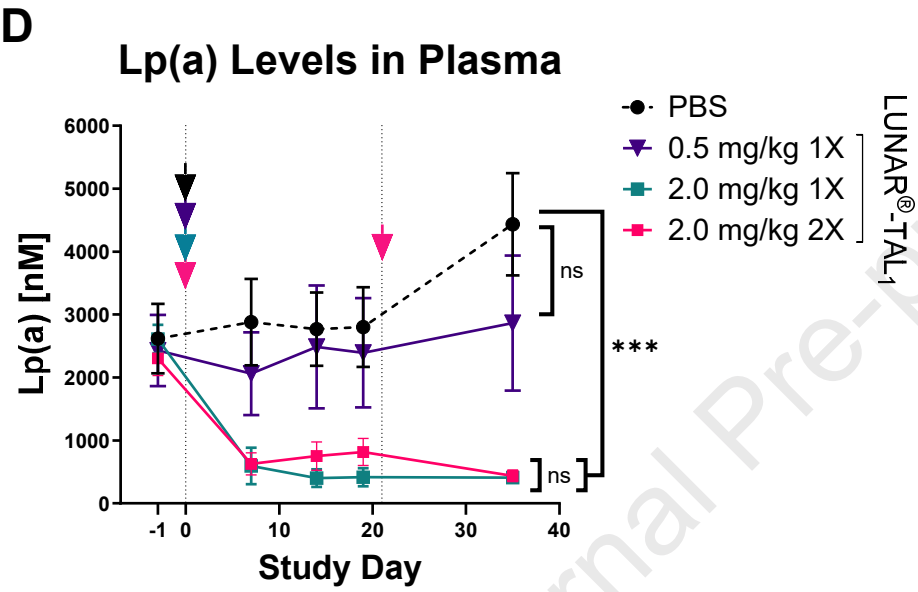

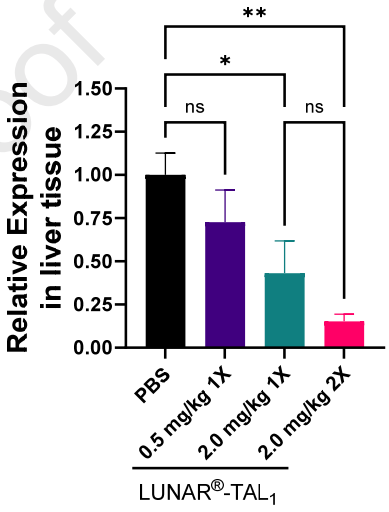

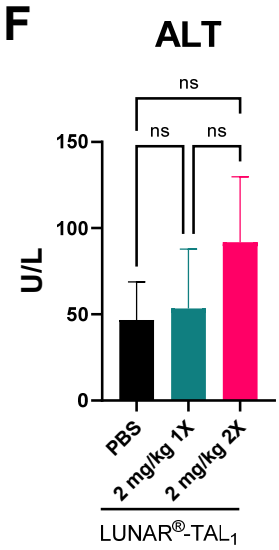

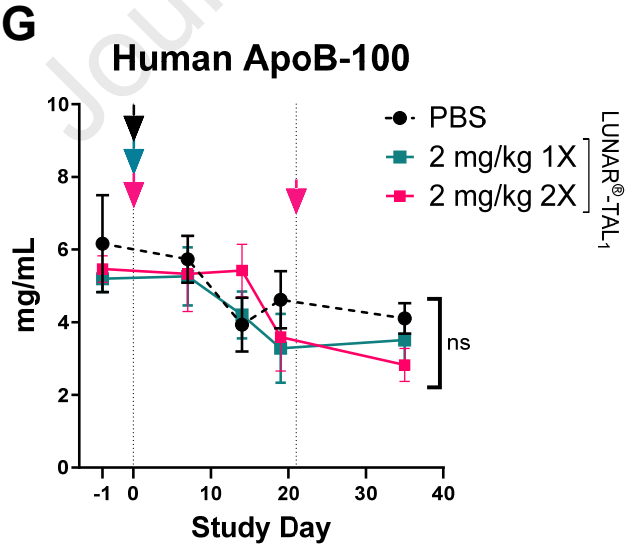

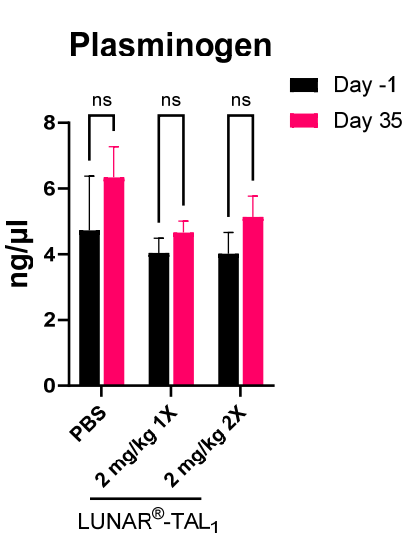

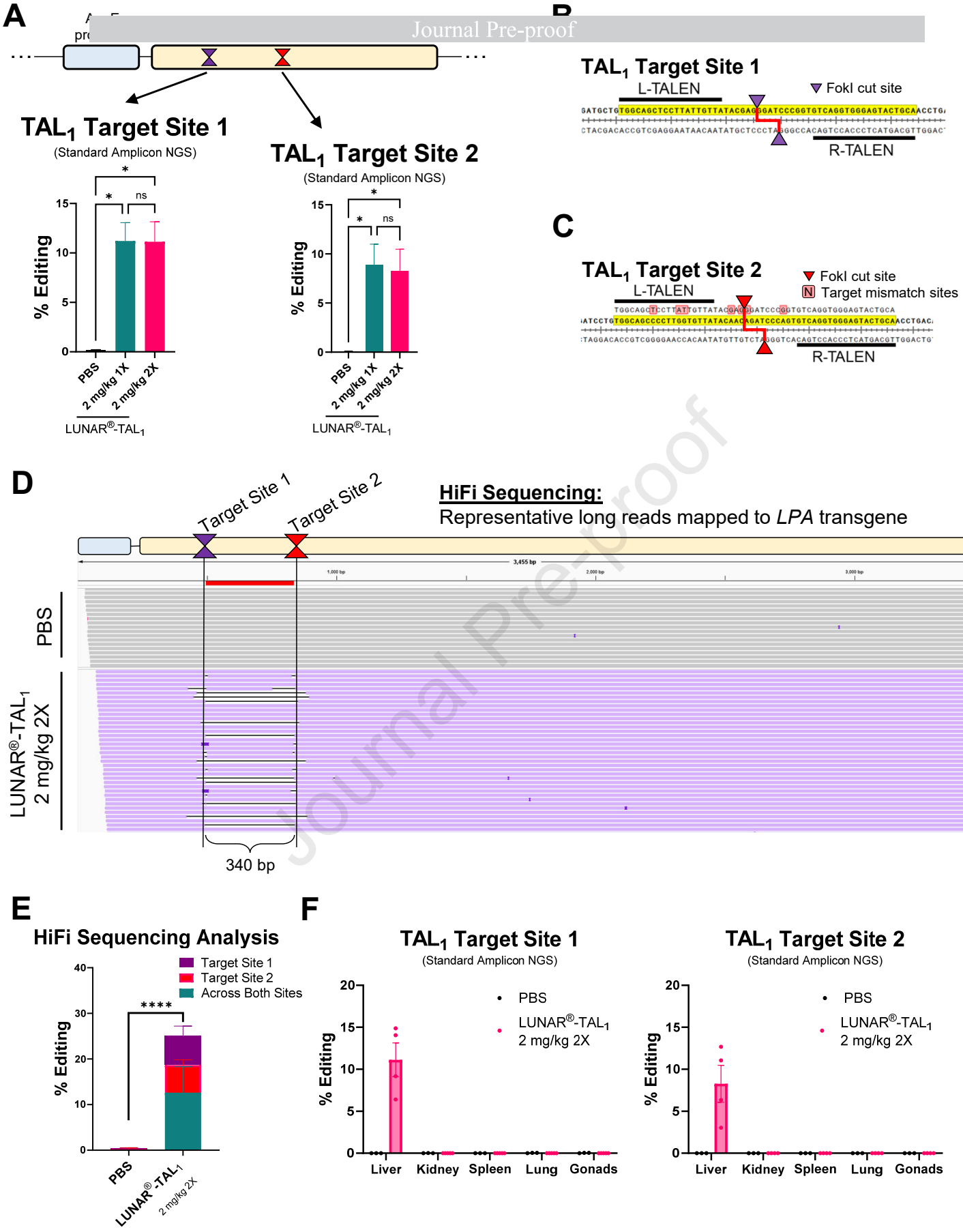

Garcia and colleagues achieved *in vivo* editing of the *LPA* gene using TALENs encoded by mRNAs encapsulated in LNPs delivered intravenously. Lp(a) reduction was observed following a single dose in mice paving the way for a long-lasting therapy for individuals with high Lp(a), a causal risk factor for cardiovascular disease.